

Mapping of thermal plasma jet non-linear dynamics in reconstructed phase space

Jan GRUBER, Jan HLÍNA, Jiří ŠONSKÝ

Institute of Thermomechanics of the ASCR, v. v. i., Dolejškova 5, 182 00 Praha 8, Czech Republic

(Received: 29 August 2008 / Accepted: 6 February 2009)

Thermal plasma jet optical radiation was observed by arrays of optical fibers and by a high-speed CCD camera. We then use the method of time-embeddings for reconstruction of dc plasma torch dynamics in the reconstructed phase space. Different properties of the plasma flow dynamics and dependence of this dynamics on input conditions (gas flow rate) are then described. We focused on non-linear and chaotic phenomena and tried to estimate the correlation dimension related to the (supposed) strange attractor of the dynamics. Sufficient spatial resolution allowed us to map the distribution of this estimated correlation dimension in different areas of the plasma jet and to compare it with the distribution of significant oscillations. This offers alternative method to describe the dynamics and provides strong tool for the analysis of the stability of plasma torch working conditions.

Keywords: thermal plasma, correlation dimension, non-linear dynamics, phase space, plasma jet, oscillations

1. Introduction

Thermal plasma jets are experimental systems which afford (according to the turbulence stage) experimental data characterized by a changing portion of regular, chaotic and noise components. Their characterization by the correlation dimensions could become an interesting tool for further investigations of turbulence and transition to turbulence in various experimental conditions. Thermal plasma is due to its specific characteristics used in variety of technological applications such as plasma spraying, plasma etching, metal welding, high-energy chemistry, material synthesis, high-temperature combustion, testing of materials, etc. The most common devices for the generation of thermal plasma jets (called plasmatrons or plasma torches) use dc-fed electric arcs for heating and ionizing the flowing gas media. Strong gradients of temperature, velocity and density in the generated plasma flow lead to the turbulent phenomena influencing the involved technological processes. A better knowledge of these effects, which can cause instability of conditions and bad reproducibility of the processes, is desirable for their future development [1-3].

Phenomena in electric arc and plasma flow follow partly periodic and partly chaotic dynamics, which leads to the modulation of the plasma optical radiation and arc voltage and current. This also strongly depends on experimental conditions (gas flow rate, feeding current). Our previous results, based on the Fourier transform and wavelet analysis, show that there are different kinds of harmonic oscillations or (generally) periodic phenomena on different time scales and that they expose specific spatial configurations [4]. We have shown that the method

of time-embedding experimental data in a reconstructed phase space is also applicable to the optical records, records of the arc current and is able to represent process dynamics and reflect stability of this dynamics [5,6].

It has been shown in the recent years that dynamics of many processes driven by the laws of deterministic chaos have, despite their complexity, a strange attractor of fractional low-dimension [7,8]. We assume such attractor in our dynamics too and we use our records and reconstructed phase portraits to estimate its correlation dimension. Results confirm previous observations (of reconstructed phase portraits) that a low-dimensional dynamics exists. More importantly, our estimated correlation dimension converges quite reasonably with embedding dimension for records from the jet core and its changes reflect changes in process dynamics. For more turbulent records from the jet boundary region the convergence is violated, however the resulting estimated correlation dimension still behaves reasonably. In this paper, we analyze the records from photodiodes for different plasmatron input parameters. We also present spatial distribution of the estimated correlation dimension for CCD records with comparison to spatial distribution of significant oscillations of the plasma jet.

2. Experimental arrangement and data evaluation

In the first experiment, the radiation of the arc and plasma jet was projected on the face areas of linear arrays of optical fibers with diameter 1 mm (each array formed by 15 elements). It was then recorded by photodiodes (Fig. 1).

In the second experiment, the jet was recorded by high-speed CCD camera (Fig. 1).

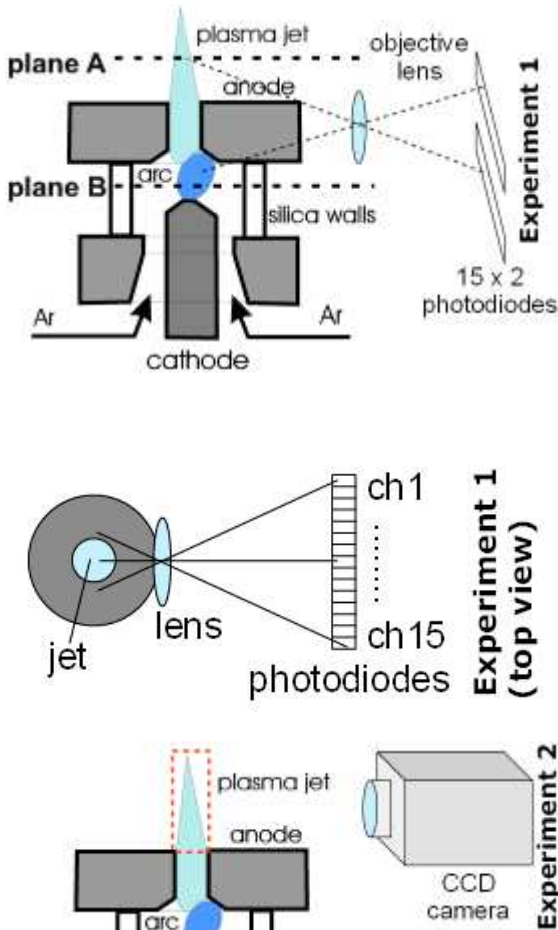


Fig 1. – Arrangement of the both experiments

Sampling frequency of the recorded data was 468.75 kHz for the photodiodes and 100 kHz for the CCD camera. We used 1 million samples of the photodiode record (for each channel) and 135000 frames of camera record. Data were processed in MATLAB computing environment.

We used the method of time-embeddings for reconstructing phase portraits of the measured process dynamics. Data are “embedded” into a reconstructed phase space by using time-delayed coordinates. *Dimension of this phase space is called embedding dimension.* This method is thoroughly described e.g. in [9]. In our previous work we estimated appropriate time lag to be 1.25 ms [6]. We have used this time lag in the experiments described in this paper too. We divide each record into subsequent chunks and try to estimate correlation dimension (fractal dimensionality of the underlying attractor) for each chunk (Fig. 2). This is necessary due to changing dynamics even within one record and allows better robustness. Each chunk is normalized to the interval <0,1> and then we use the method based on Grassberger-Procaccia algorithm [10,11] to estimate the correlation dimension. Classical algorithm uses all the (N * (N-1)) point pairs of phase portrait.

$$C(r) = \frac{2}{N(N-1)} \sum_{j=1}^N \sum_{i=j+1}^N O(r - r(i, j)) \quad , \quad (1)$$

where $r(i,j)$ is distance calculated by the Euclidean norm and O is Heaviside function.

We use slight modification based on pseudorandomly choosing only fixed number ($n * n$) of point pairs. We then calculate the correlation sum as stated.

For each chunk and for each embedding dimension we get some dependency of correlation sum $C(r)$ on the radius of hypersphere. The slope of this dependency in some scaling region approximates the correlation dimension. We have found that the number of 400*400 points is sufficient to catch the slope in the scaling region whereas being almost 100 times faster to calculate than using all the points. Embedding dimension goes from 2 to 16 and logarithm of r spans equidistantly interval (-2, 0) by 201 points. Scaling region of logarithm of r was chosen the same (-1.4, -0.4) for all the data. Therefore we can compare estimated correlation dimensions together. Because reasonable convergence of estimated correlation dimension with growing embedding dimension is hard to achieve for our data, we use mean of the estimates along some interval of embedding dimensions (usually 4 to 16) as our “estimated correlation dimension” (cD). However, we also keep record of “maximum estimate(d) correlation dimension along embedding dimensions” and “minimum estimate(d) correlation dimension along embedding dimensions” for the reference and for the information how good our “(mean) estimated correlation dimension” is [6] (Fig. 3a,b).

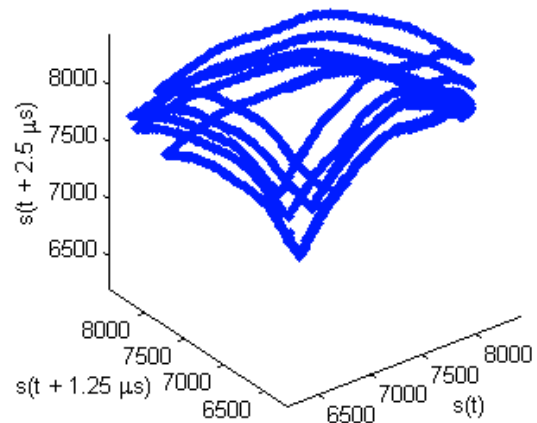


Fig 2. – Sample chunk of data embedded into reconstructed phase space. (time lag 1.25ms, embedding dimension 3), data of the arc radiation – channel 6

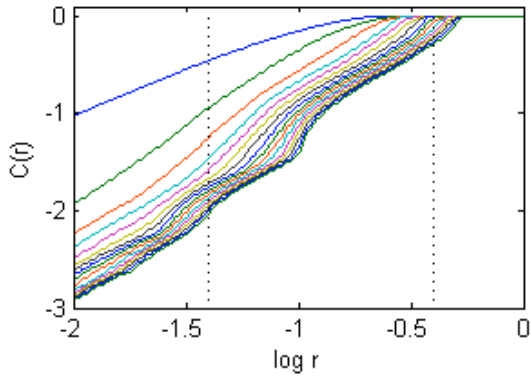


Fig 3a. – Plot of correlation sums (for embedding dimensions 1 to 16 – different colored lines), (same data as in Fig. 2), emphasized interval: $\log r = (-1.4, -0.4)$

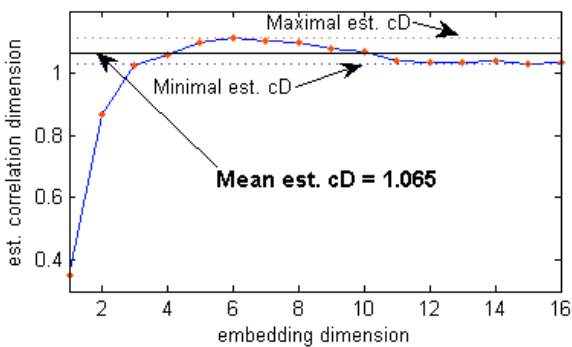


Fig 3b. - Plot of estimated correlation dimension (max-mean-min emphasized), (same data as in Fig. 2)

The example in Fig. 3b is example of a very nice convergence. Usually the plot of estimated correlation dimension continues to rise or even rises to some maximum and then for higher embedding dimensions decreases again. However we can still calculate the mean along embedding dimensions and compare this number for different areas of the plasma jet.

Spectral analysis of the data was done by standard FFT algorithm. We used all 135000 frames and calculated the power spectral density (PSD) for (signal in) each CCD element. By summation of these PSDs in interesting frequency intervals, we get distribution of the specific oscillations in the CCD-recorded plane [4].

3. Results

In Fig. 4 we can see sample evolution of profile of the plasma arc (recorded inside the plasmatron, plane B in Fig. 1) and of profile of the plasma jet (recorded outside the plasmatron, plane A in Fig. 1). In Fig. 5 we can see several frames recorded by a CCD camera and mean from all the 135000 frames.

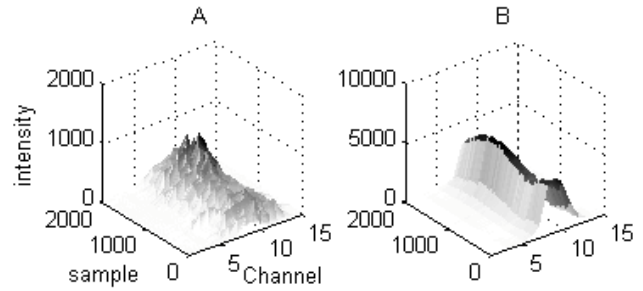


Fig 4. – Part of photodiodes record (argon flow rate 1 g/s, mean current 164 A, 2000 samples, A – plasma jet, B – arc)

Mean frame represents the overall radiation intensity of the jet and sample frames illustrate that the dynamics of the jet is quite vivid, especially in the boundary layer.

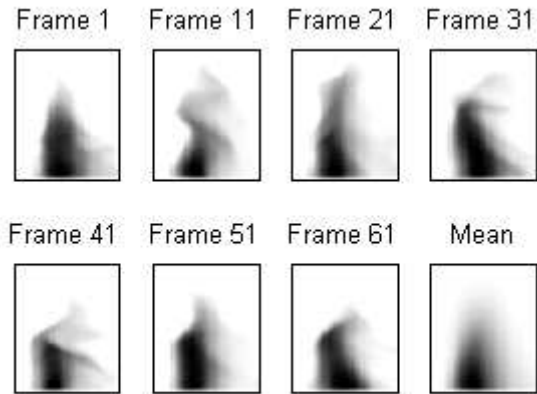


Fig 5. – Sample CCD frames and mean frame (argon flow rate 1 g/s, frame time lag 0.1 ms)

There are some distinct oscillations in the optical radiation. Low-frequency oscillations, which are electric in origin, exhibit themselves mostly in the jet core. Higher frequency oscillations are present in the boundary layer where mixing with the external air and turbulent phenomena occur (Fig.6).

If we use CCD records and explore spatial distribution of oscillations in the specific frequency intervals, we can confirm that high-frequency oscillations occur mostly in the jet shear layer (Fig. 7). This is interesting to compare with later distribution of cD (Fig. 12).

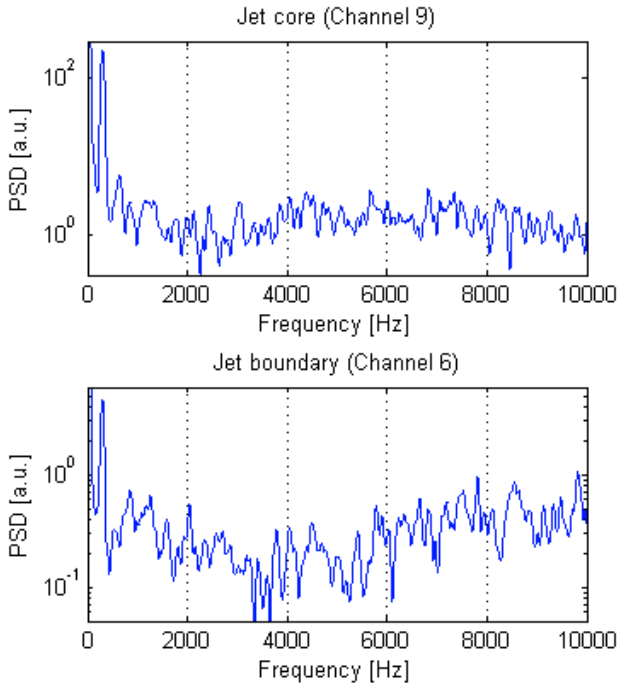


Fig 6. – Power spectral density calculated from photodiodes record of plasma jet. (Welch method, argon flow rate 1 g/s, mean current 164 A, 40 ksamples)

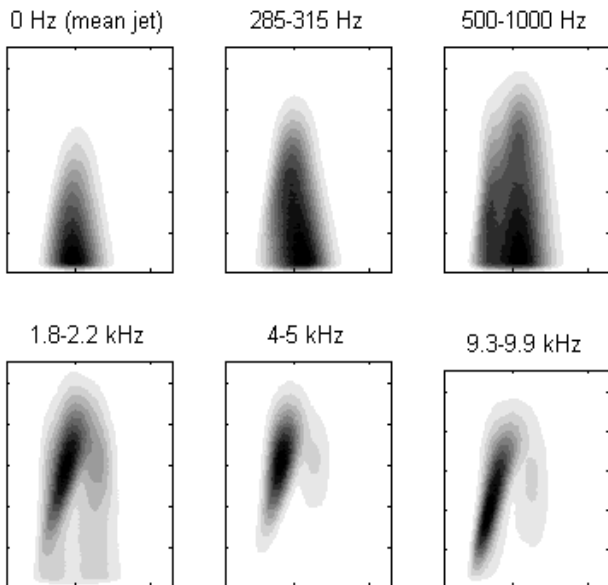


Fig 7. – Distribution of oscillations in the plasma jet in specific frequency intervals (Argon flow rate 0.7 g/s, $|FFT|^2$ from 135 ksamples)

Estimated correlation dimension (cD) reflects complexity of the underlying dynamics. By dividing the whole record from the photodiodes into 100 chunks (10000 points per chunk) and estimating cD for each chunk, we can see that this complexity changes slightly and decrease of cD in the boundary channels on one side is *coincident* with increase in the boundary channels on the other side. (Fig. 8) That can probably be ascribed to some travelling structures behind the oscillations that change position in somewhat radial motion. We would need longer records to confirm that pattern.

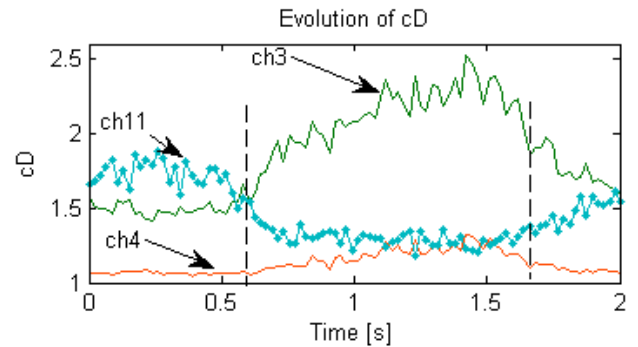


Fig 8a. – Evolution of estimated correlation dimension of optical records from different channels of the arc (argon flow rate 0.5 g/s, mean current 109A)

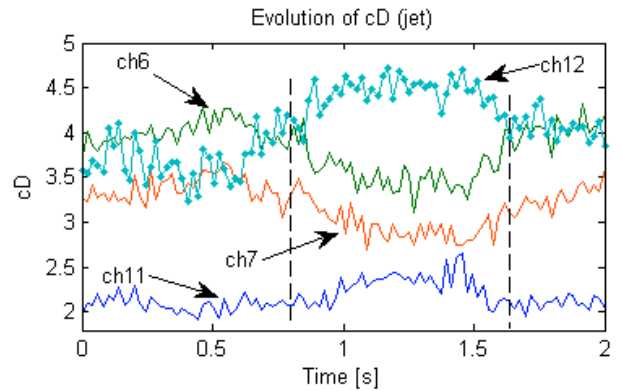


Fig 8b. – Evolution of estimated correlation dimension of optical records from different channels of the jet (argon flow rate 0.5 g/s, mean current 109A)

Although cD varies during the record, it is generally higher in the boundary channels (where mixing with an external air and turbulent phenomena occur) and lower in the middle (core) channels. If we take a mean of cD along all the chunks, we can see this profile (Fig. 9). We also plot “maximum estimated correlation dimension” for the reference. Interesting result is that in the arc axis there is a small rise of the estimated correlation dimension. This should indicate that the most stable region of the arc is actually at some small distance from the arc axis.

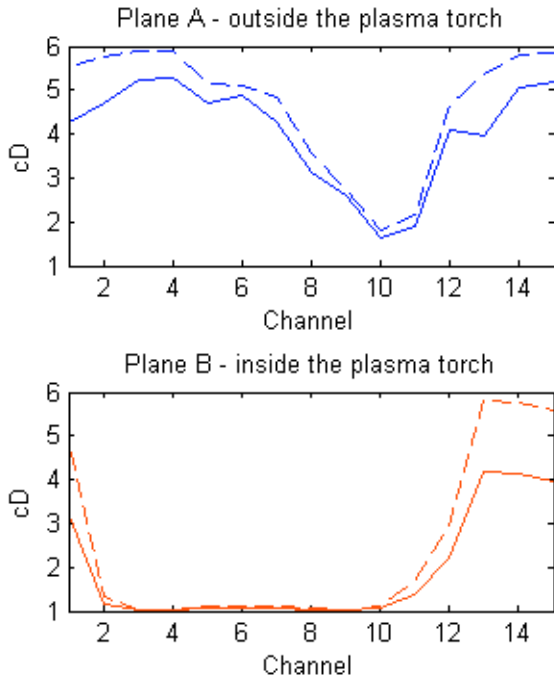


Fig 9. – Profiles of estimated correlation dimension and „maximum estimated correlation dimension“ (argon flow rate 0.5 g/s, mean current 154 A)

We have undertaken time-consuming calculation of cD in each point of the CCD record to map this distribution in the whole recording plane. For the time reasons, we used just the first 10000 samples. The results for two different argon flow rates are in Fig. 10 and Fig. 11. Zero results from the outer region are quite irrelevant, because the signal there is rather sporadic, consisting of occasional shots of jet radiation. By better visualizing the distribution (Fig. 12), we can see where the turbulent phenomena really concentrate. In general, it is higher in the boundary region and the jet core is more stable. However this distribution does not possess any simple symmetry, differs for each gas flow rates and can hardly be reduced to some simple geometry. It seems that there are actually two additional layers (one with higher cD and one with lower cD) between stable core and unstable boundary for gas flow rate 0.7 g/s and helix-like structure for 1.5 g/s.

Higher gas flow rate leads to the overall increase of cD and the layer of high cD (indicating turbulent behavior) is more complex. Sometimes structures are better visible on the plots of “minimum cD” and “maximum cD”, however it is the mean cD, which should be considered as the best approximation of real estimated correlation dimension.

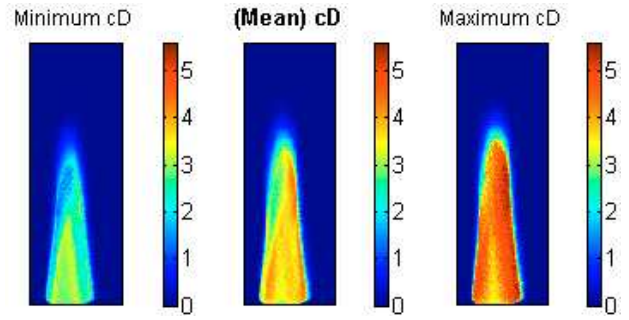


Fig 10. – Distribution of estimated correlation dimension in the recording plane (argon flow rate 0.7 g/s)

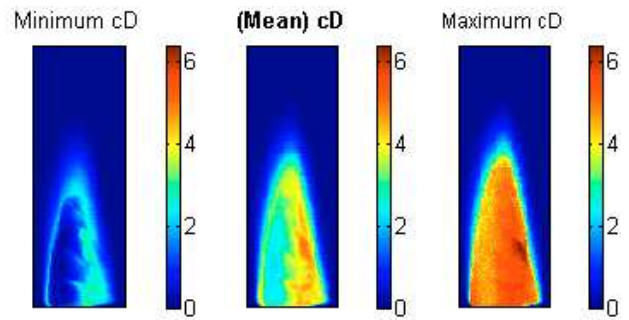


Fig 11. – Distribution of estimated correlation dimension in the recording plane (argon flow rate 1.5 g/s)

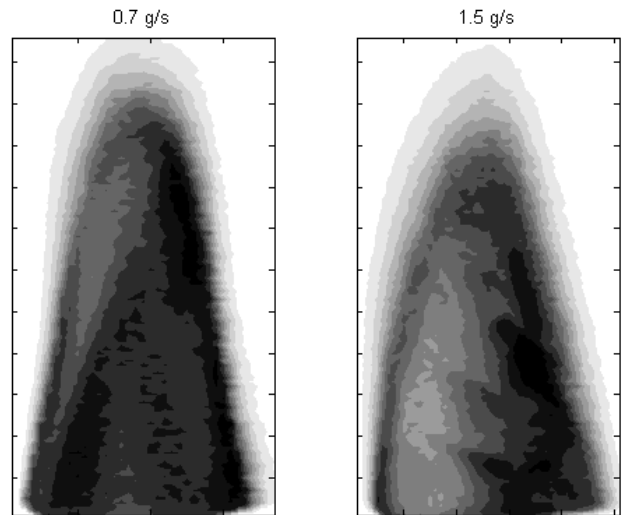


Fig 12. – More detailed view at distribution of correlation dimension (both argon flow rates, darker tones means higher cD)

4. Conclusion

We have used a method based on Grassberger-Procaccia algorithm to estimate correlation dimensions for the records of plasma arc and plasma jet optical radiation. In the arc core, the estimated correlation dimension is slightly above 1. In the plasma jet core it is between 1.5 – 3. In the boundary regions it rises above 4 and due to the poor convergence we should not call this number “correlation dimension” there. However, we have mapped the distribution of this estimate in the arc profile and the jet profile and in the plane of the jet. Results show that estimated correlation dimension reflects degree of chaoticity and turbulence in the jet, being higher in the boundary mixing region and lower in the jet core. They also indicate that there are probably several layers in the plasma jet according to cD or even more complicated structures. It also seems that the most stable region of the plasma arc is not exactly at the arc core. Correlation dimension estimates also confirm that higher gas flow rate leads to a more turbulent dynamics. Comparison with distribution of distinct oscillations shows that significant and therefore stable oscillations lead to a lower estimated correlation dimension, but the distribution of specific frequency oscillations does not catch turbulent region in such complexity as cD does.

This method of estimating correlation dimension can therefore be used as an alternative indicator of stability of processes in a plasma flow, to map the turbulence and similar phenomena and to characterize plasma jet dynamics.

- [1] S. Ghouri *et al.*, IEEE Trans. Plasma Sci. **34**, 121 (2006).
- [2] J. Heberlein, Pure Appl. Chem. **74**, 327 (2002).
- [3] P. Fauchais and A. Vardelle, Plasma Phys. Control. Fusion **42**, B365 (2000).
- [4] J. Hlína, J. Gruber, and J. Šonský, in *Proceedings of the 17th International Symposium on Plasma Chemistry* (Toronto, Canada, Aug. 7–15, 2005), pp. 353–354.
- [5] J. Hlína, J. Gruber, J. Šonský, and J. Šlechta, Acta Techn. CSAV **52**, 109 (2007).
- [6] J. Hlína, J. Gruber, and J. Šonský, Acta Techn. CSAV **52**, 321 (2007).
- [7] J.H. Yeom, T. Rhee, and C.M. Ryu, Jpn. J. Appl. Phys. **45**, 6486 (2006).
- [8] M.A. Hassouba *et al.*, Phys. Plasmas **13**, 073504 (2006).
- [9] H.D.I. Abarbanel *et al.*, Rev. Mod. Phys. **65**, 1331 (1993).
- [10] P. Grassberger and I. Procaccia, Phys. Rev. Lett. **50**, 346 (1983).
- [11] Julien Clinton Sprott, *Chaos and Time-Series Analysis* (Oxford University Press, New York, 2003), pp. 307–310.